SCIENCE CHINA
Technological Sciences

October 2010 Vol.53 No.10: 2708–2717
doi: 10.1007/s11431-010-4075-4

Multi-objective robust airfoil optimization based on non-uniform rational B-spline (NURBS) representation

LIANG Yu, CHENG XiaoQuan*, LI ZhengNeng & XIANG JinWu

School of Aeronautic Science and Engineering, Beihang University, Beijing 100191, China

Received May 12, 2010; accepted July 5, 2010

In order to improve airfoil performance under different flight conditions and to make the performance insensitive to off-design condition at the same time, a multi-objective optimization approach considering robust design has been developed and applied to airfoil design. Non-uniform rational B-spline (NURBS) representation is adopted in airfoil design process, control points and related weights around airfoil are used as design variables. Two airfoil representation cases show that the NURBS method can get airfoil geometry with max geometry error less than 0.0019. By using six-sigma robust approach in multi-objective airfoil design, each sub-objective function of the problem has robustness property. By adopting multi-objective genetic algorithm that is based on non-dominated sorting, a set of non-dominated airfoil solutions with robustness can be obtained in the design. The optimum robust airfoil can be traded off and selected in these non-dominated solutions by design tendency. By using the above methods, a multi-objective robust optimization was conducted for NASA SC0712 airfoil. After performing robust airfoil optimization, the mean value of drag coefficient at *Ma*0.7−0.8 and the mean value of lift coefficient at post stall regime (*Ma*0.3) have been improved by 12.2% and 25.4%. By comparing the aerodynamic force coefficients of optimization result, it shows that: different from single robust airfoil design which just improves the property of drag divergence at *Ma*0.7−0.8, multi-objective robust design can improve both the drag divergence property at *Ma*0.7− 0.8 and stall property at low speed. The design cases show that the multi-objective robust design method makes the airfoil performance robust under different off-design conditions.

robust design, multi-objective optimization, NURBS, Pareto front, airfoil

Citation: Liang Y, Cheng X Q, Li Z N, et al. Multi-objective robust airfoil optimization based on non-uniform rational B-spline (NURBS) representation. Sci China Tech Sci, 2010, 53: 2708−2717, doi: 10.1007/s11431-010-4075-4

1 Introduction

In traditional airfoil design optimization, designers usually concentrate on aerodynamic performance at certain design point (or called flight condition). The limitation of this traditional method is that, when the flight condition departs from design point, aerodynamic performance may be deteriorated significantly. For example, with the increase of Mach number in transonic region, airfoil drag coefficient increases dramatically. By using multi-point optimization method, better performance at a given set of design points can be achieved, however, unsatisfactory performance losses over the entire range of flight conditions still exist [1]. Therefore, a method which can develop aerodynamic performance at main design points and avoid sudden depravation in off-design conditions should be developed. To make optimum result insensitive to the off-design flight conditions, various robust design methods have been adopted [2−6] in airfoil design. Because of the complication of multi-objective design problem, only a few researches have been performed on robust airfoil design considering multi-

*Corresponding author (email: xiaoquan_cheng@buaa.edu.cn)

ple flight conditions.

In this paper, six-sigma robust approach was expanded to multi-objective design problem by combining a genetic algorithm based on non-dominated sorting. The multi-objective robust airfoil design approach was proposed and applied to airfoil design. Six-sigma approach [4] expresses robust design problem the same as optimization process. It was used to describe sub-objective function in multi-objective optimization design problem. A multi-objective genetic algorithm was used to obtain a set of optimum airfoils called "non-dominated front". The optimum airfoil considering robustness can be selected from this non-dominated front. To reduce computation cost, Kriging approximation model was used to replace CFD analysis during optimization process.

In order to describe airfoil geometry by design variables, airfoil parameterization must be involved in optimization. It needs a representation method to satisfy the accuracy requirement with a few design variables. Non-uniform rational B-spline (NURBS) parameterization method uses control points as design variables [7]. Applying NURBS representation to airfoil robust design will also be discussed here.

2 Derivation of multi-objective robust airfoil optimization problem

2.1 Six-sigma robust design

Robust design is defined as the design, which is insensitive to external noises or tolerances [2]. It can be classified into Taguchi method, robust optimization and robust design with the axiomatic approach. The robust design formulation is written as follows:

$$\text{find:} \quad \boldsymbol{x} \in \boldsymbol{R}^n, \tag{1}$$

$$\text{minimize:} \quad F(\boldsymbol{x}, \boldsymbol{p}, \boldsymbol{z}), \tag{2}$$

$$\text{subject to:} \quad G_j(\boldsymbol{x}, \boldsymbol{p}, \boldsymbol{z}) \leqslant 0,\ j = 1 \cdots r, \tag{3}$$

$$\boldsymbol{x}_L \leqslant \boldsymbol{x} \leqslant \boldsymbol{x}_U,$$

where $\boldsymbol{x}$ is the design variable vector and $\boldsymbol{p}$ is the design parameter vector which is usually regarded as constant during design process. A noise factor $\boldsymbol{z}$ is an additional term in the robust design functions, which is different from normal optimization problem.

In eq. (2), objective function F can also be expressed as $f(\boldsymbol{x}+z^x, \boldsymbol{p}+z^p)$, and noise factor $\boldsymbol{z}$ is divided to $\boldsymbol{z}^x$ (the noise vector of $\boldsymbol{x}$)and $\boldsymbol{z}^p$ (the noise vector of $\boldsymbol{p}$) respectively. In eq. (3) G_j is the constraint of robust design, like objective function, it can be rewritten as $\mathrm{g_j}(\boldsymbol{x}+z^x, \boldsymbol{p}+z^p)$.

In order to consider the performance development as well as the insensitivity to the noise in eq. (2), mean value μ_f and variance σ_f^2 are proposed. The formulation can be expressed as follows [2]:

$$\begin{aligned}\mu_f &= E\left[f(x)\right] \\ &= \iint \cdots \int f(\boldsymbol{x}+z^x, \boldsymbol{p}+z^p) u_1\left(z_1^x\right) \cdots u_{\mathrm{n}}\left(z_{\mathrm{n}}^x\right) \\ &\quad \times v_1\left(z_1^p\right) \cdots v_{\mathrm{m}}\left(z_{\mathrm{m}}^p\right) \mathrm{d}z_1^x \cdots \mathrm{d}z_{\mathrm{n}}^x \mathrm{d}z_1^p \cdots \mathrm{d}z_{\mathrm{m}}^p,\end{aligned} \tag{4}$$

$$\begin{aligned}\sigma_f^2 &= E\left[f(x) - \mu_f\right]^2 \\ &= \iint \cdots \int \left\{f(\boldsymbol{x}+z^x, \boldsymbol{p}+z^p) - \mu_f\right\}^2 \mathrm{u}_1\left(z_1^x\right) \cdots u_{\mathrm{n}}\left(z_{\mathrm{n}}^x\right) \\ &\quad \times v_1\left(z_1^p\right) \cdots v_{\mathrm{m}}\left(z_{\mathrm{m}}^p\right) \mathrm{d}z_1^x \cdots \mathrm{d}z_{\mathrm{n}}^x \mathrm{d}z_1^p \cdots \mathrm{d}z_{\mathrm{m}}^p,\end{aligned} \tag{5}$$

where $u_i(z_i^x)$ and $\boldsymbol{v}_i(z_i^p)$ are the probability density functions.

Six-sigma method expresses robust problem as the combination of mean value and standard deviation; it belongs to robust optimization. Compared with other robust design approaches, six-sigma approach is relatively easy to apply in optimization problem. In six-sigma approach, μ_f and σ_f^2 are formulated as a single objective function [4], which is shown as

$$\text{minimize:} \quad w_\mu \mu_f + w_\sigma \sigma_f^2, \tag{6}$$

where w_μ and w_σ are weight factors. The values of these factors are specified by the user.

Eq. (6) needs to satisfy a quality constraint:

$$\begin{aligned}\mu_f - n\sigma_f &\geqslant \mathrm{LSL}, \\ \mu_f + n\sigma_f &\leqslant \mathrm{USL},\end{aligned} \tag{7}$$

where USL and LSL are upper and lower bounds of acceptable solution. n is user defined sigma level which refers to robustness quality. For larger value of n, the robustness quality is better. The default value of sigma lever n is 6.

2.2 Description of robust airfoil design based on six-sigma approach

The disturbance of flight condition may unpredictably deteriorate the performance of airfoil [7, 8]. Therefore, it is necessary to make the airfoil insensitive to the disturbance. In order to describe typical multi-objective robust airfoil design problem, two flight conditions are considered in this paper. One is cruise condition in transonic regime and the other is take-off/climbing condition at low speed. Both of them are the important flight segments of transport jet. Corresponding to these conditions, two parameters are considered as uncertain variables: Mach number Ma and angle of attack α.

Assuming Ma and α follow certain distribution in the range $[Ma_{\min}, Ma_{\max}]$ and $[\alpha_{\min}, \alpha_{\max}]$. The probability den-

sity function are defined as $v[Ma]$ and $v[\alpha]$. Two aerodynamic parameters are treated as objective performance: the drag coefficient under a given cruise lift coefficient and lift coefficient near stall regime at low speed. The mean and variance of two aerodynamic characteristics can be expressed as follows: for low speed flight condition, max lift coefficient C_{lmax} is considered, then,

$$\begin{aligned}\mu_{C_{\mathrm{lmax}}} &= \int_{\alpha_{\min}}^{\alpha_{\max}} C_{\mathrm{l}}(D,\alpha)v(\alpha)\mathrm{d}\alpha,\\ \sigma^2_{C_{\mathrm{lmax}}} &= \int_{\alpha_{\min}}^{\alpha_{\max}} (C_{\mathrm{l}}(D,\alpha)-\mu_{C_{\mathrm{l}}})^2 v(\alpha)\mathrm{d}\alpha\end{aligned} \tag{8}$$

for transonic flight condition, drag coefficient C_{d} is considered, then,

$$\begin{aligned}\mu_{C_{\mathrm{d}}} &= \int_{M_{a\min}}^{M_{a\max}} C_{\mathrm{d}}(D,Ma,\alpha)v(Ma)\mathrm{d}Ma,\\ \sigma^2_{C_{\mathrm{d}}} &= \int_{M_{a\min}}^{M_{a\max}} \left(C_{\mathrm{d}}(D,Ma,\alpha)-\mu_{C_d}\right)^2 v(Ma)\mathrm{d}Ma\end{aligned} \tag{9}$$

Based on six-sigma approach in ref. [5], the airfoil robust design problem can be developed and be formulated as for low speed flight condition

minimize: $$-w_\mu\mu_{C_{\mathrm{l}}}+w_\sigma\sigma^2_{C_{\mathrm{l}}}, \tag{10}$$

subject to: $$\mu_{C_{\mathrm{l}}}-n\sigma^2_{C_{\mathrm{l}}} > LSL_{C_{\mathrm{l}}};$$

for transonic flight condition

minimize: $$w_\mu\mu_{C_{\mathrm{d}}}+w_\sigma\sigma^2_{C_{\mathrm{d}}}, \tag{11}$$

subject to: $$\mu_{C_{\mathrm{d}}}+n\sigma^2_{C_{\mathrm{d}}} < USL_{C_{\mathrm{d}}},$$

$$C_l\left(\boldsymbol{x},Ma,\alpha\right) \geqslant C_{\mathrm{l}}^* \quad (\text{for} \quad Ma_{\min} \leqslant Ma \leqslant Ma_{\max}),$$

where C_{l}^* is given lift coefficient in transonic regime.

2.3 Derivation of multi-objective robust airfoil design problem

Usually airplane has different mission segments such as take-off, climb and cruise, etc. In order to satisfy the practical requirement in robust airfoil design, it is necessary to consider different flight conditions. An efficient multi- objective optimization approach containing robust objective functions is required. The multi-objective optimization problem can be written as follows:

minimize: $$\boldsymbol{\varphi}(\boldsymbol{x})=[\phi_1(\boldsymbol{x}),\phi_2(\boldsymbol{x}),\cdots,\phi_n(\boldsymbol{x})], \tag{12}$$

subject to:

$$\boldsymbol{x}\in R^m=\left\{\boldsymbol{x}\middle| g_j(\boldsymbol{x})\leqslant 0, j=1,2,\cdots,p\right\},$$

where $\varphi(\boldsymbol{x})$ is the vector of multi-objective functions and $g_i(\boldsymbol{x})$ is the constraint.

In multi-objective robust airfoil design process, $\phi_i(\boldsymbol{x})$ represents the sub-object of robust airfoil. Therefore, the robust objective function in each flight condition (eqs. (10) and (11)) can be treated as sub-objective function: $\phi_i(\boldsymbol{x})$ in eq. (12). The multi-objective robust airfoil design problem can be expressed as

minimize: $$\boldsymbol{\varphi}(\boldsymbol{x})=[\phi_1(\boldsymbol{x}),\phi_2(\boldsymbol{x})],$$

where $$\phi_1(\boldsymbol{x})=-w_\mu\mu_{C_{\mathrm{l}}}+w_\sigma\sigma^2_{C_{\mathrm{l}}},$$

$$\phi_2(\boldsymbol{x})=w_\mu\mu_{C_{\mathrm{d}}}+w_\sigma\sigma^2_{C_{\mathrm{d}}}$$

subject to:

1) $\boldsymbol{x_L}\leqslant\boldsymbol{x}\leqslant\boldsymbol{x}_U$,

2) for $\phi_1(\boldsymbol{x})$: $\mu_{C_{\mathrm{l}}}-n\sigma^2_{C_{\mathrm{l}}} > LSL_{C_{\mathrm{l}}}$,

3) for $\phi_2(\boldsymbol{x})$: $\mu_{C_{\mathrm{d}}}+6\sigma^2_{C_{\mathrm{d}}} < USL_{C_{\mathrm{d}}}$,

$$C_{\mathrm{l}}(\boldsymbol{x},Ma,\alpha)\geqslant C_{\mathrm{l}}^*.$$

Multi-objective optimization methods are adopted to solve this problem. The methods can be classified into two types: weighted sum method and non-dominated optimization method. Weighted sum method combines the multi-objective functions into a linear aggregating function. It changes multi-objective problem into a single-object optimization process. The disadvantage of this traditional method is that, if the design tendency is changed, the optimum result needs to be recalculated. In contrast to weighted sum method, non-dominated optimization method can give a set of non-dominated solutions [9]. The non-dominated solutions represent the multi-objective optimum results with different design tendencies. Therefore, the optimum solution can be selected by tradeoff on these non-dominated solutions. Non-dominated solutions can be defined as: if and only if there is no solution $\boldsymbol{U}$, the solutions satisfy the following equation:

$$\forall i,\ \ \phi_i(\boldsymbol{U})\leqslant\phi_i(\boldsymbol{V}) \tag{13}$$

$$\exists i,\ \ \phi_i(\boldsymbol{U})<\phi_i(\boldsymbol{V}),\ \ \ i=1,2,\cdots n,$$

where $\boldsymbol{U},\boldsymbol{V}\in R^m$. The vector $\boldsymbol{V}$ is called non-dominated solution or Pareto solution.

By using non-dominated algorithm, the process of multi-objective robust airfoil design is defined as finding optimum airfoil geometries to obtain all non-dominated solutions (Pareto front). In order to meet the requirement of multi-objective airfoil design and consider robust problem in each design object, a non-dominated multi-objective genetic algorithm—NSGAII [10] is adopted. In NSGAII, fitness is calculated by non-dominated sorting and crowding distance sorting. There are two advantages of NSGAII: the fast non-dominated sorting method can reduce the computa-

tion complexity to $O(MN^2)$; diversity preservation is obtained by introducing crowd comparison operator, it avoids defining sharing function. As compared to other methods, NSGAII is able to obtain better spread of solutions and has better convergence near the true Pareto-optimal front. The detailed optimization process using NSGAII will be discussed in Section 4.

3 NURBS airfoil representation

In order to describe airfoil geometry by design variables, a representation method is required. Different types of representation methods are available such as PARSEC method, Hicks-Henne method and NURBS method [11, 12]. Different from the two former methods, NURBS method can express complex and the detailed shape of geometry by using control points and related weights as design variables. NURBS representation has natural smoothness [13], it can avoid suffering noise and "bump". A pth-degree NURBS curve is defined as [14]

$$\boldsymbol{C}(u)=\sum_{i=0}^{n}R_{i,p}(u)\boldsymbol{P}_i,\quad a\leqslant u\leqslant b;$$

$$R_{i,p}(u)=\frac{N_{i,p}(u)w_i}{\sum_{j=0}^{n}N_{j,p}(u)w_i},\quad a\leqslant u\leqslant b, \tag{14}$$

where $\{\boldsymbol{P}_i\}$ are the control points with coordinates (x_i, y_i). $\{w_i\}$ is the weight of control point. u is relative position of the curve, and it usually has the value between [0, 1]. $\{N_{i,p}(u)\}$ is the pth-degree B-spline basis functions.

$N_{i,p}(u)$ is founded by knot vector $U=\left(\underbrace{a,\cdots,a}_{p+1},u_{p+1},\cdots,u_{m-p-1},\underbrace{b,\cdots,b}_{p+1}\right)$, and can be calculated by the following equations:

$$N_{i,0}(u)=\begin{cases}1 & \text{if } u_i\leqslant u<u_{i+1},\\ 0 & \text{otherwise,}\end{cases}$$

$$N_{i,p}(u)=\frac{u-u_i}{u_{i+p}-u_i}N_{i,p-1}(u)+\frac{u_{i+p+1}-u}{u_{i+p+1}-u_{i+1}}N_{i+1,p-1}(u). \tag{15}$$

Instead of parameterization of the airfoil into single curve, more accurate airfoil geometry can be achieved by separating the airfoil into upper and lower NURBS curves [15, 16]. The representation is shown in Figure 1. The first and ending control points are fixed in the leading and tailing edges of airfoil. Seven control points are distributed along each curve. In ref. [16], only the coordinates of control point are considered as design variables, the error of representation may become relatively large because the weight of control point is not changed. Therefore, the weight parameter w_i is also introduced as design variable in this paper. Then the design variables of parameterization include the coordinates (x_i, y_i) and the weight w_i of control points.

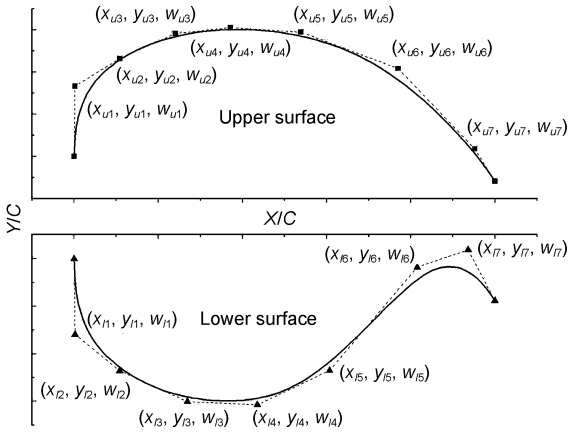

Figure 1 Representation and design variables of NURBS.

In order to obtain the appropriate weight and distribution of control points, an optimization for representation problem needs to be conducted. The representation error between original airfoil and representation geometry can be expressed by mean value ε_{mea} and max value $\varepsilon_{\max}$ [7]:

$$\varepsilon_{\text{mea}}=\frac{1}{k}\sum_{j=1}^{k}\frac{d_j}{C}, \tag{16}$$

$$\varepsilon_{\max}=\max\left(\frac{d_j}{C}\right),\quad 1\leqslant j\leqslant k,$$

where d_j is the distance between target curves and their projections in original airfoil, C is the chord length of airfoil, k is the number of the points which are used to calculate ε_{mea} and $\varepsilon_{\max}$ on the airfoil. In this research, 100 points distributed uniformly along airfoil are selected and the value of k is set to be 100. The representation optimization problem then can be written as follows:

$$\text{minimize:}\qquad F(\boldsymbol{x}_{\text{af}})=2\varepsilon_{\text{mea}}+\varepsilon_{\max}, \tag{17}$$

where x_{af} is the coordinate vectors of control points, and $\boldsymbol{x}_{\text{af}}=\{x_1,y_1,w_1,\cdots,x_n,y_n,w_n\}$.

Two different types of airfoil: NASA SC(2)-0712 and NACA 64(1)-212 were introduced to validate NURBS representation method. Gradient based optimization was adopted to solve the distribution problem. The representation results and weight values are shown in Figure 2. By using NURBS method, the geometries after representation match well with original airfoils. The max error $\varepsilon_{\max}$ is less than 0.0019 and mean error ε_{mea} is less than 0.0007.

4 Flow solution and optimization process

4.1 Flow solution

In airfoil design, an appropriate method is required to solve

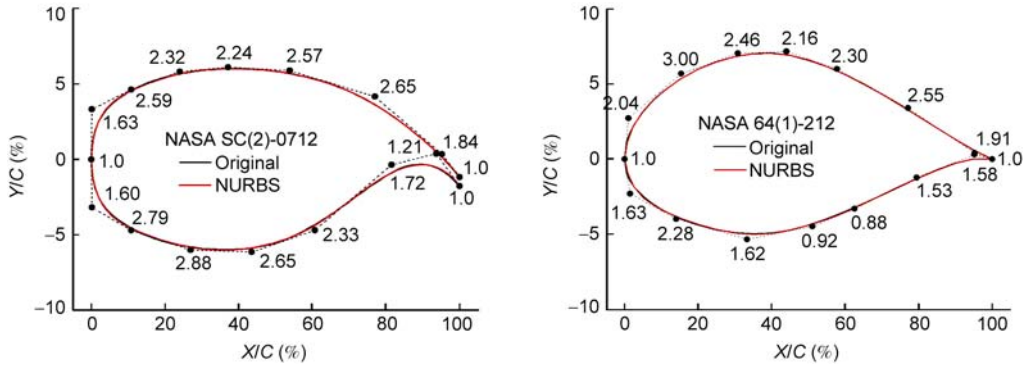

Figure 2 Comparison of NURBS geometry and original airfoil.

the complex flow problems. These problems include shock effect in transonic regime, flow separation at high angle of attack, etc. Linear aerodynamic estimation methods (such as panel method) can give accurate result only in certain flight conditions, such as cruise condition at low speed. By integrating limited volume in entire flow space, Navier-Stokes solver of CFD can describe the complex flow and get accurate aerodynamic forces. For this reason, Navier-Stokes solver was used to make airfoil optimization results reliable. Fluent Inc commercial software was used in the CFD computation. During the solution process, a compressible solver with second order upwind scheme was adopted, S-A one-equation turbulence model was involved to account for the viscous effect. C-H structural grid was adopted to reduce the computation cost. The grid distribution is 360 (flow direction) ×70 (normal direction). Figure 3 shows the comparison between the CFD and experiment result of RAE 2822 [17] airfoil at *Ma*0.75. It shows that the CFD result matches well with the experiment result.

4.2 Approximation model and optimization process

In robust optimization, aerodynamic forces should be computed in the flight conditions which depart from design points. It needs more computation cost than normal optimization problem. For this reason, using NS solver directly in optimization becomes unacceptable, especially in multi-objective robust design problem. In order to reduce the computation cost as well as keep fidelity of optimization result, approximation model was adopted. In contrast to other approximation methods, Kriging model has local approximation property and can achieve better results in nonlinear problems [18]. The relationship between response and variable of Kriging model can be defined as

$$y(\boldsymbol{x}) = f(\boldsymbol{x}) + Z(\boldsymbol{x}), \tag{18}$$

where $y(\boldsymbol{x})$ is unknown function, $f(\boldsymbol{x})$ is known function. $Z(\boldsymbol{x})$ is the realization of a stochastic process and needs to satisfy the following relationship of statistics:
the mean value needs to satisfy:

$$E[Z(\boldsymbol{x})] = 0, \tag{19}$$

the variance value needs to satisfy:

$$Var[Z(\boldsymbol{x})] = \sigma^2, \tag{20}$$

the covariance matrix needs to satisfy:

$$Cov[Z(\boldsymbol{x}^i), Z(\boldsymbol{x}^j)] = \sigma^2 \boldsymbol{R}[R(\boldsymbol{x}^i, \boldsymbol{x}^j)]. \tag{21}$$

In eq. (21), $\boldsymbol{R}$ is correlation matrix, and $R(\boldsymbol{x}^i, \boldsymbol{x}^j)$ is the correlation function between two of the sampled data points $\boldsymbol{x}^i$ and $\boldsymbol{x}^j$. More detailed expression of functions and the predicted estimates can be found in ref. [18].

In robust design process, Kriging model is used to approximate the relationship between aerodynamic forces (solved by CFD) and design variables. By replacing CFD analyses in the optimization process, Kriging model can reduce computation cost and keep the reliability of aerodynamic forces. The flow chart of multi-objective robust airfoil optimization is shown in Figure 4. First, the airfoil is parameterized into design variables by NURBS representation. Then Latin-Hypercubes design of experiment (DOE) is used to select the most important parameters and these

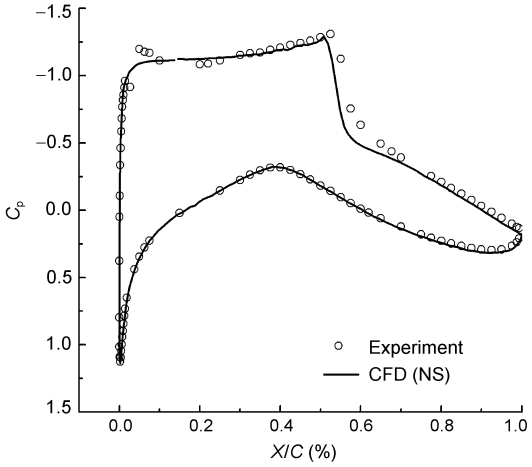

Figure 3 CFD validation of RAE 2822.

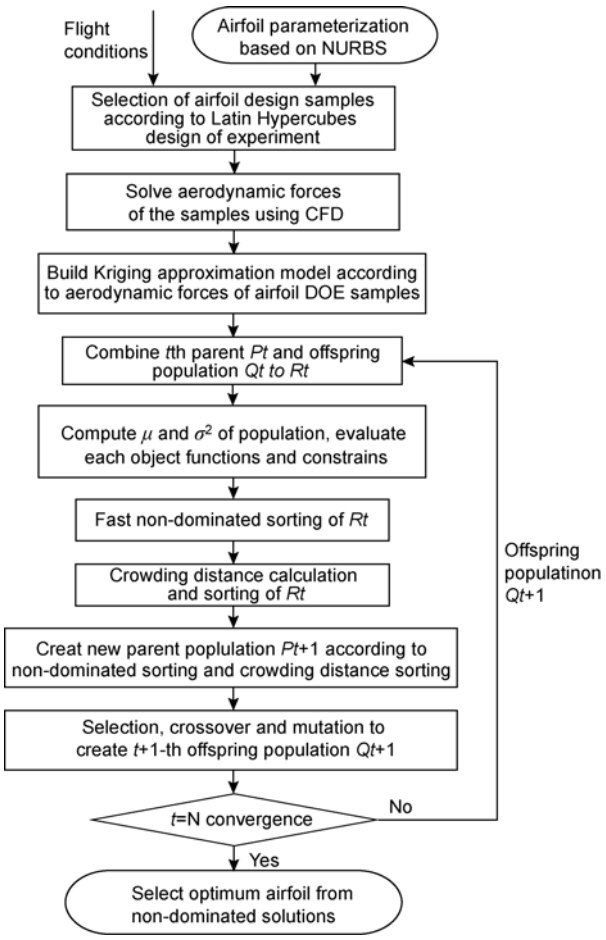

Figure 4 Flow chart of airfoil robust optimization.

parameters are treated as design variables, the details of the selection method can be found in ref. [19]. From the design space founded by design variables, a set of sample airfoils is selected by the DOE method. Based on the CFD results of the sample airfoils, Kriging model is formulated. From the Kriging model, the aerodynamic forces of feasible solutions are obtained and used to calculate each robust objective function. Multi-objective genetic algorithm NSGAII computes non-dominated solutions and generates next generation until the ending rule is satisfied. Finally, according to the design tendency, the optimum airfoil can be selected from the non-dominated solutions.

5 Examples of robust airfoil design

In aircraft design, cruise drag during transonic cruise as well as max lift during takeoff/climbing influences the performance of transport jet significantly [20]. In this paper, robust airfoil design considers these two aerodynamic forces. A super critical airfoil, NASA SC(2)-0712 [21], is selected as the original airfoil. By Latin-Hypercubes DOE, 13 parameters were selected as design variables, which are shown in Figure 5. Also by using DOE, 169 (13^2) airfoil geometries were selected as design samples. These samples were used to formulate approximation model. According to the property of NASA SC(2)-0712, the range of cruise *Ma* is usually between 0.7 and 0.8 , and α near/post stall regime is between 12° and 16° at *Ma*0.3. The random variable *Ma* and α are assumed to be distributed in the regime uniformly. Therefore, [*Ma*=0.7, 0.72, 0.74, 0.76, 0.78, 0.8] in transonic regime and [α=12°, 13°, 14°, 15°, 16°] at *Ma*0.3 were treated as the samples of *Ma* and α. The mean and variance values of aerodynamic performance in eqs. (8) and (9) can be simplified to statistics formulation:

a) For low speed flight condition, eq. (8) can be simplified to

$$\begin{aligned}\mu_{C_{1\max}} &\approx \frac{1}{n_{\text{low}}}\sum_{k=1}^{n_{\text{low}}}\hat{C}_1(D,\alpha_k),\\ \sigma^2_{C_{1\max}} &\approx \frac{1}{n_{\text{low}}-1}\sum_{k=1}^{n_{\text{low}}}\left(\hat{C}_1(D,\alpha_k)-\mu_{C_1}\right)^2,\end{aligned} \tag{22}$$

where $\hat{C}_1(D,\alpha_k)$ is the lift coefficient of α samples, and n_{low} is the number of α samples.

b) For transonic flight condition, eq. (9) can be simplified to

$$\begin{aligned}\mu_{C_d} &\approx \frac{1}{n_{\text{tran}}}\sum_{k=1}^{n_{\text{tran}}}\hat{C}_d\left(D,Ma_k,\alpha\right),\\ \sigma^2_{C_d} &\approx \frac{1}{n_{\text{tran}}-1}\sum_{k=1}^{n_{\text{tran}}}\left(\hat{C}_d(D,Ma,\alpha)-\mu_{C_d}\right)^2,\end{aligned} \tag{23}$$

where $\hat{C}_d(D,Ma,\alpha)$ is the drag coefficient of *Ma* samples and n_{tran} is the number of *Ma* samples.

Two robust optimization cases are discussed here. These cases correspond to single-object and multi-objective robust optimization respectively. The precision of Kriging model calculated at multi-objective optimum point is shown in Table 1. The absolute value of force coefficient error is less than 7% and the absolute value of objective function error is less than 5%; the precision of Kriging model can meet the requirement of robust airfoil design.

5.1 Case 1: Robust airfoil optimization with single object

NASA SC(2)-0712 has lower drag coefficient than lots of other airfoils when Mach number is below 0.75. When the

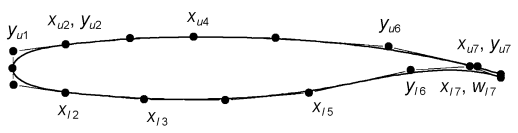

Figure 5 Design variables of NASA SC(2)-0712.

Table 1 Validation of Kriging model (multi-objective optimum solution)

Design object 1 (low speed regime)	Performance	C_l (at α=12°)	C_l (at α=14°)	C_l (at α=16°)	$\mu_{C_l}+\sigma^2_{C_l}$
	Kriging prediction	1.778	1.541	0.999	1.576
	result from CFD	1.781	1.651	1.056	1.614
	prediction error (%)	−0.18	−6.66	−5.40	−2.34
Design object 2 (transonic regime)	performance	C_d (at Ma=0.70)	C_d (at Ma=0.74)	C_d (at Ma=0.78)	$\mu_{C_d}+\sigma^2_{C_d}$
	Kriging prediction	0.0138	0.0154	0.0206	0.0195
	result from CFD	0.0141	0.0146	0.0213	0.0203
	prediction error (%)	−2.04	5.54	−3.29	−4.02

speed exceeds the critical Mach number, the drag caused by shock wave increases significantly. It is expected to develop an airfoil that has lower drag coefficient and is insensitive to Mach number. In this robust design problem, Mach number is treated as uncertain variable, and optimization problem is described as

$$\text{minimize: } \mu_{C_d}+\sigma^2_{C_d},$$

$$\text{subject to: } \mu_{C_d}+6\sigma^2_{C_d}<0.04,$$

where the weights of mean and variance are set to be 1.0.

In optimization process, the drag coefficient was calculated at the given lift coefficient C_l=0.7. Kriging models were constructed corresponding to each case of [Ma=0.7, 0.72, 0.74, 0.76, 0.78, 0.8]. Multi-island genetic algorithm was adopted to solve this single-object optimization problem. The population size is 100 (10 islands and 10 population in each island) and the max number of generations is 40.

After optimization, the objective function has been improved by 16.48%, the mean value of the result is 0.01908 and the variance value is 3.29×10^{-5}. Figure 6 shows the transonic drag comparison between the optimum and original airfoils (solved by CFD). The drag coefficient of optimum airfoil is reduced significantly in the regime Ma0.75−0.8. The drag plot in the entire range becomes 'flat', although the drag is a little larger than original airfoil in the regime below Ma0.75. In other words, after robust optimization, the drag becomes insensitive to Mach number. Figure 7 shows the geometries of optimum and original airfoils. The upper surface of optimum airfoil becomes flat and the lower surface near tailing edge becomes more concave. This geometry can delay the critical shock wave and reduce its intensity, which is shown in Figure 8.

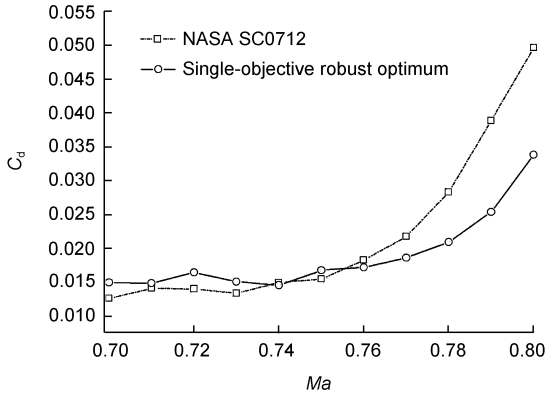

Figure 6 Drag coefficient comparison (CFD) between original and single-objective robust airfoils in Ma0.7− 0.8.

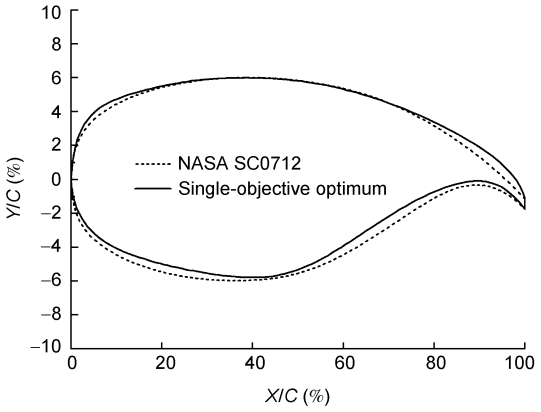

Figure 7 Geometry of single-objective optimum robust airfoil.

5.2 Case 2: Robust airfoil optimization with multi-object

Besides the drag of transonic cruise condition, max lift coefficient of takeoff/climbing conditions is another important aerodynamic performance. Large lift coefficient means short takeoff distance and high climbing rate. According to the viewpoint of control and stability, sudden drop of the lift coefficient in near/after stall regimes should be avoided. Improving lift coefficient in α=12°−16° as well as reducing the lift sensitivity to α formulates another robust design object. Multi-objective robust design problems related to takeoff/climbing and transonic cruise flight conditions are conducted here. The design problem can be expressed as:

$$\text{minimize: } \boldsymbol{\varphi}(\boldsymbol{x})=[\phi_1(\boldsymbol{x}),\phi_2(\boldsymbol{x})],$$

$$\text{where } \phi_1(x)=-\mu_{C_l}+\sigma^2_{C_l},$$

$$\phi_2(x)=\mu_{C_d}+\sigma^2_{C_d},$$

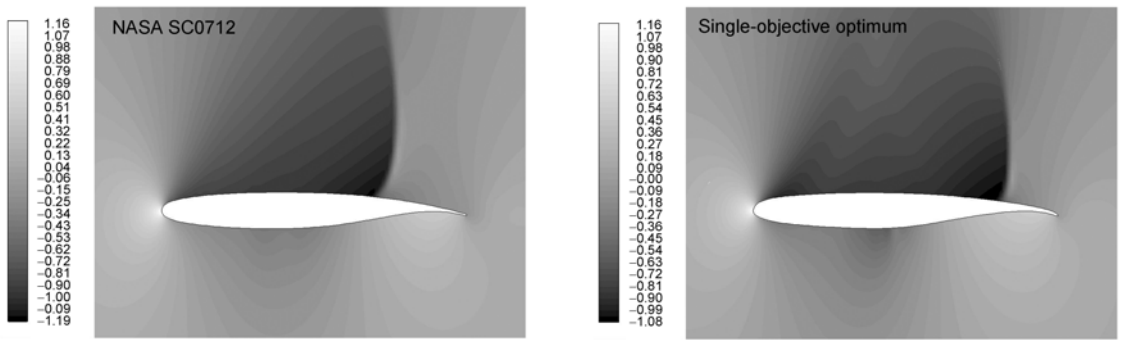

Figure 8 The critical shock wave of original airfoil and single-objective optimum robust airfoil (CFD, pressure coefficient at *Ma*0.79).

objective functions subject to:

$$\mu_{C_l} - 6\sigma_{C_l}^2 > 0.8,$$
$$\mu_{C_d} + 6\sigma_{C_d}^2 < 0.04.$$

As the design process shown in Figure 4, NSGAII was used to solve this multi-objective problem. The population size is 100, and the number of generation is 60. Figure 9 shows the non-dominated result (Pareto front) obtained by NSGAII. For multi-objective optimization, the optimum solution is actually a tradeoff between multi-objectives in Pareto front and optimum airfoil can be selected from this Pareto front. In this case, the objective function of transonic drag $\phi_2(x)$ is relatively more important than $\phi_1(x)$, therefore, the optimum solution which tends to transonic object $\phi_2(x)$ was selected as multi-objective robust airfoil.

The performance comparisons are shown in Figures 10 and 11 (solved by CFD), where the single-objective optimization result obtained from Case 1 is also included in Figures 10 and 11, in order to compare the difference between single-objective and multi-objective optimization results. In near/post stall regime, the lift coefficient of multi-objective optimum has been improved significantly. In comparison to the original airfoil whose lift drops suddenly after stall, the lift coefficient of multi-objective optimum airfoil can sustain high value from α=12° to α=13.5° and drops smoothly after 13.5°. Similar to the result in Case 1, in transonic regime, the drag coefficient of multi-objective optimum has been reduced in the range of *Ma*0.75–0.8, which makes the optimum airfoil more insensitive to Mach number.

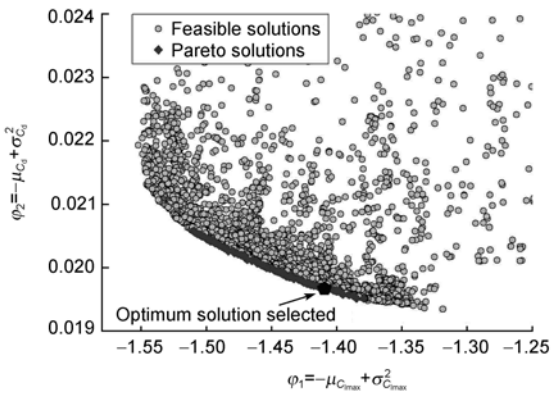

Figure 9 Pareto front and optimum selection in multi-objective robust design.

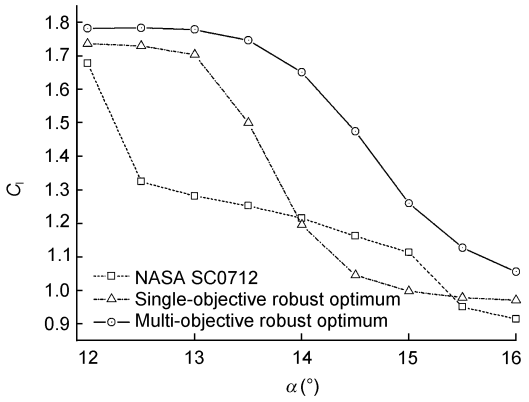

Figure 10 Lift coefficient comparison (CFD) in stall regime between robust airfoil and original airfoil (*Ma*0.3).

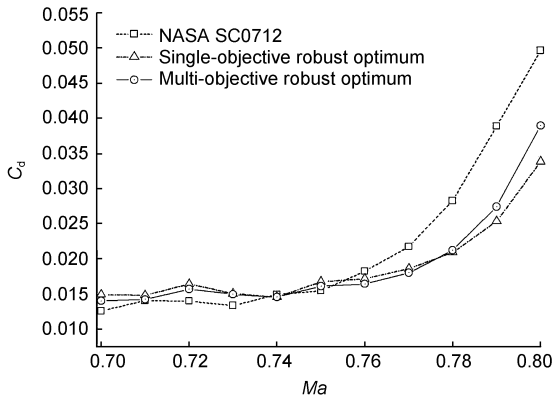

Figure 11 Drag coefficient comparison (CFD) between robust airfoil and original airfoil in *Ma*0.7–*Ma* 0.8.

The optimum geometry of multi-objective robust design is shown in Figure 12. Similar to single-object robust design

result, the optimum of multi-objective design has flat upper surface, and more concavity at tailing edge of lower surface; the upper curve near leading edge of multi-objective airfoil is smoother than that of single-object airfoil. This geometry results in weaker shock wave and smaller separation regime, which is shown in Figures 13–15.

In contrast to single-objective optimum, the drag coefficient of the multi-objective optimum is a little higher than that of the single-objective optimum. The reason can be found from the difference of control points' parameters and geometries between two optimums, which is shown in Figure 12. For multi-objective optimum airfoil, one of the object functions is to develop the robustness of lift coefficient in near/after stall regime at low speed. So after optimizing the controls points' parameters, the curvature near the leading edge of the upper surface becomes smoother than that of the single-objective airfoil (Figure 12). This smoother leading edge delays the separation at low speed, which is shown in Figure 14. But for the drag coefficient at *Ma*0.7–0.8, this smoother leading edge also causes the loss of negative pressure coefficient near the leading edge of upper surface, which is shown in Figure 15. This loss of

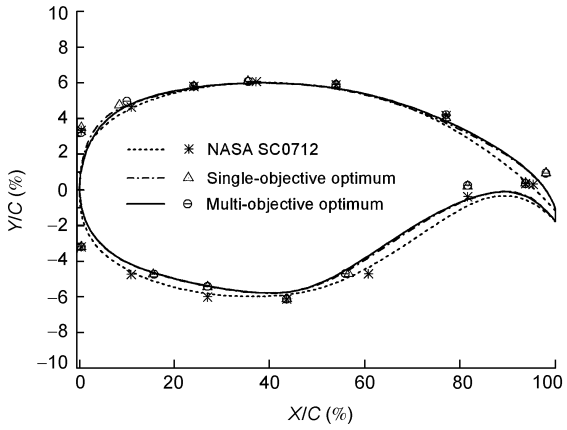

Figure 12 Airfoil geometry and control points of multi-objective robust design optimization.

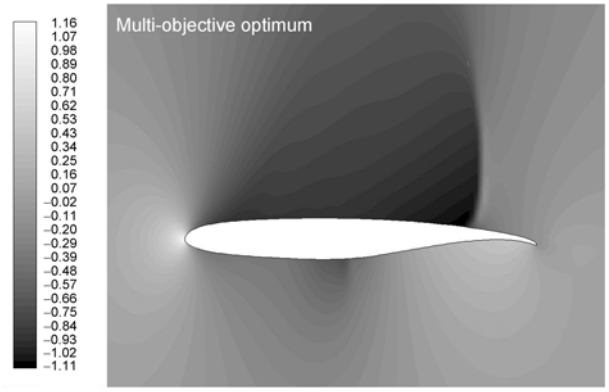

Figure 13 The critical shock wave of multi-objective optimum airfoil (pressure coefficient at *Ma*0.79, CFD).

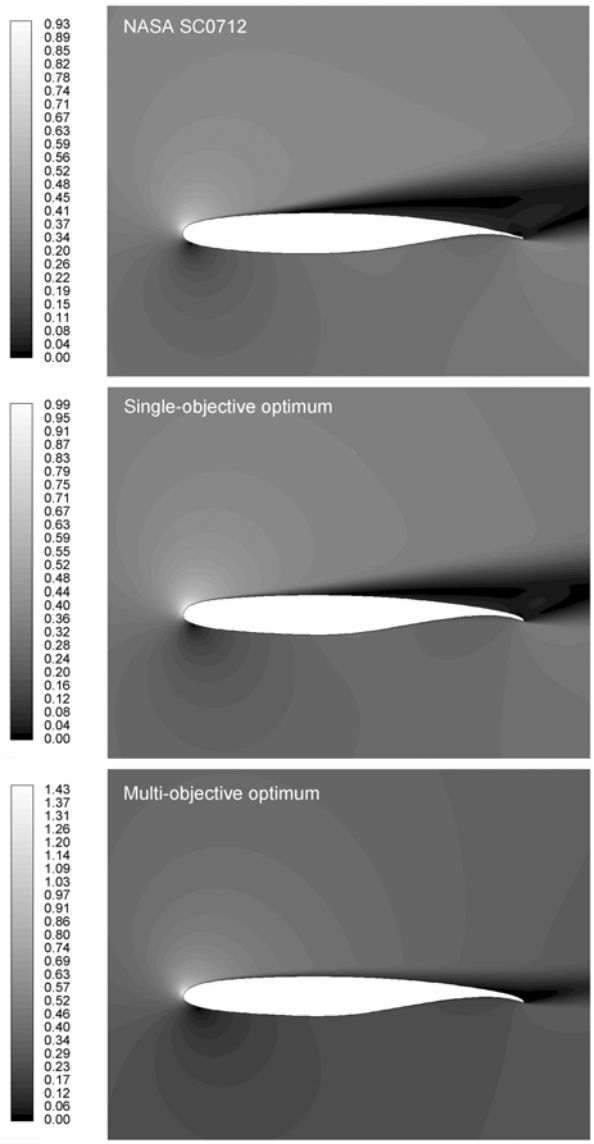

Figure 14 Comparison of stall regime between original and optimum airfoils (α=14°, *Ma*=0.3, Mach number distribution, CFD).

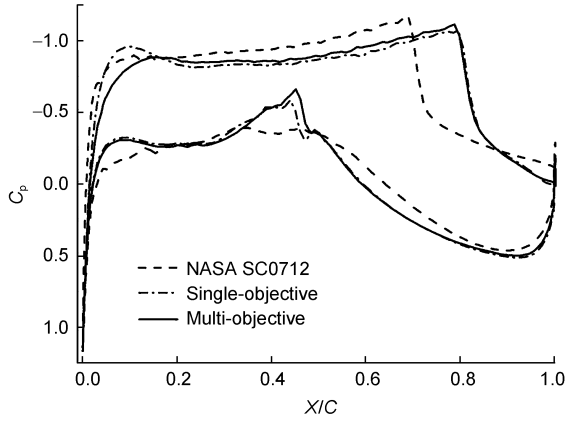

Figure 15 The pressure coefficient of airfoils at *Ma*0.79 (CFD).

pressure coefficient near leading edge makes the drag coefficient a little higher than single-objective optimum. The aerodynamic character of the design case reflects the trade-off essence of multi-objective optimization.

6 Conclusion

Multi-objective robust design approach has been developed and applied to airfoil design optimization. Two robust airfoil design cases were studied and investigated. These cases proved the effectiveness of the approach. The multi-objective robust airfoil design has the following characteristics:

(1) In multi-objective problem, six-sigma approach is adopted in each objective function. The approach makes the optimum solution have robustness property. Because six-sigma approach expresses robust design problem as optimization process, it is convenient to be combined with multi-objective optimization.

(2) By NURBS representation method, airfoil geometry with $\varepsilon_{\max}$ less than 0.0019 can be obtained using small number of design variables. It is important in airfoil optimization.

(3) Non-dominated genetic algorithm can obtain non-dominated front (Pareto front) of optimum solution. Robust airfoil can be chosen by tradeoff between design objects on non-dominated front.

(4) Kriging approximation model can reduce the computation cost incurred due to random variables. Optimization results have shown the effectiveness of Kriging model.

By using multi-objective robust design approach, an optimum airfoil was successfully developed from original airfoil NASA SC0712. The improvement of aerodynamic performance in low speed and transonic flight conditions can be obtained. At the same time, six-sigma approach makes the results more insensitive to undesired changes of flight conditions.

In future work, the influence of weight factors' value on six-sigma approach will be investigated. Other flight conditions should be considered in the robust airfoil design. In addition, advanced applications such as multi-objective robust wing design are also expected.

1 Painchaud-Ouellet S, Tribes C, Trépanier J Y, et al. Airfoil shape optimization ouUsing NURBS representation under thickness constraint. AIAA 2004-1095, 2004
2 Park G J, Lee T H, Lee K H, et al. Robust design: An overview. AIAA J, 2006, 44(1): 181−191
3 Li W, Huyse L, Padula S, et al. Robust airfoil optimization to achieve consistent drag reduction over a Mach range. NASA/CR-2001-211042, 2001
4 Shimoyama K, Oyama A, Fujiii K. Development of multi-objective six-sigma approach for robust design optimization. J Aerospace Comp, Inf Comm, 2008, 5(8): 215−233
5 Shimoyama K, Oyama A, Fujii K. Multi-objective six sigma approach applied to robust airfoil design for Mars airplane. AIAA 2007-1966, 2007
6 Zhong X P, Ding J F, Li W J, et al. Robust airfoil optimization with multi-objective estimation of distribution algorithm. Chinese J Aeronaut, 2008, 21(4): 289−295
7 Lepine J, Guibault F, Trepanier J Y. Optimized nonuniform rational B-spline geometrical representation for aerodynamic design of wings. AIAA J, 2001, 39(11): 2033−2041
8 Hager J O, Eyi S, Lee K D. Multi-point design of transonic airfoils using optimization. AIAA 92−4225, 1992
9 Coello C, Lamont G, Veldhuizen D. Evolutionary Algorithms for Solving Multi-objective Problems. Stanford: Springer, 2007. 62−91
10 Deb K, Pratap A, Agarwal S, et al. A fast and elitist multiobjective genetic algorithm: NSGA-II. IEEE Transactions on Evolutionary Computation, 2002, 6(2): 182−197
11 Sobieczky H. Parametric airfoils and wings. Notes Num Fluid Mech, 1998, 68: 71−88
12 Song W B, Keane A J. A Study of shape parameterisation methods for airfoil optimisation. AIAA 2004-4482, 2004
13 Lepine J, Trepanier J Y. Wing aerodynamic design using an optimized NURBS geometrical representation. AIAA 2000-0699, 2000
14 Piegl L, Tiller W. The NURBS Book. Berlin: Springer, 1995. 117–124
15 Kumano T, Jesong S, Obayashi S, et al. Multidisciplinary design optimization of wing shape for a small jet aircraft using Kriging model. AIAA 2006-932, 2006
16 Takenaka K, Obayashi S, Nakahashi K, et al. The application of MDO technologies to the design of a high performance small jet aircraft lessons learned and some practical concerns. AIAA 2005-4797, 2005
17 Cook P H, McDonald M A, Firmin M C P. Aerofoil RAE 2822-pressure distributions, and boundary layer and wake measurements. Experimental Data Base for Computer Program Assessment. AGARD Report AR 138, 1979
18 Simpson T W, Mauery T M, Korte J J, et al. Comparison of response surface and Kriging models for multidisciplinary design optimization. AIAA-98-4755, 1998
19 Koch P N, Simpson T W, Allen J K, et al. Statistical approximations for multidisciplinary design optimization: The problem of size. J Aircraft, 1999, 36(1): 275−286
20 Raymer D P. Aircraft design: a conceptual approach [M]. Washington DC: American Institute of Aeronautics and Astronautics, 1989. 451−489
21 Harris C D. NASA supercritical airfoils. NASA Technical Paper, TP-2969, 1990